

## EXPERIMENTAL AND NUMERICAL TRANSIENT THERMAL ANALYSIS OF THE IDLER BEARING HOUSING MADE OF STEEL OR POLYMER MATERIAL

by

**Marko M. TASIĆ<sup>a\*</sup>, Radivoje M. MITROVIĆ<sup>b</sup>, and Žarko Z. MIŠKOVIĆ<sup>b</sup>**

<sup>a</sup>Academy of Applied Technical Studies Belgrade,  
Department for Traffic, Mechanical, and Safety Engineering, Belgrade, Serbia  
<sup>b</sup>Faculty of Mechanical Engineering, University of Belgrade, Belgrade, Serbia

Original scientific paper  
<https://doi.org/10.2298/TSCI220429129T>

*The research of the influence of housing material on operation temperature of the idler bearing assembly is presented in this paper. Several radial loads and rotary speeds were applied to the test bench to determine the transient temperature field. The results were monitored and recorded for the whole period until the temperature of the assembly reached stationary stage. The FEM model was created where the rolling elements were replaced with the especially designed artificial body, having the shape of irregular ring. It generates heat and connects only those points of the inner and outer ring which are in operating conditions connected with the rolling elements. The experimental results are compared with FEM results. The conclusion is given on suitability of polymer material for this purpose.*

Key words: *radial ball bearings, transient temperature field, finite element analyses*

### Introduction

Polymer materials are being used more frequently in modern constructions. Due to their light weight and affordable price, polymer parts enable easier manipulation during maintenance process. Maintenance can be done much faster, which shortens the dead lock period of the facility, and enables higher productivity of electricity. Moreover, lighter construction of conveyor systems enables easier start of the system and reduces electricity consumption of the production facility [1], which leaves more electricity for consumers.

This scientific paper presents an experiment whose purpose is to answer the question of the impact of housing material, radial load, and rotation speed on transient temperature field in the bearing, housing and shaft. Harris [2] gives the theoretical way to calculate quantity of generated heat and total heat flow for the given operating conditions, but it does not provide answer on how to calculate temperature at a specific point of the assembly after a specific period of time. Živković *et al.* [3] defined analytical model of heat transfer which enables to define influence of rotary speed and temperature (among other constructive and

---

\*Corresponding author, e-mail: mtasic@atssb.edu.rs

technological parameters) on static and dynamic characteristics of the bearing and its' life time. Azianou *et al.* [4] replaced balls with contact elements to estimate the influence of housing deformation on load distribution zone. Kushwaha *et al.*[5] solved a similar problem of heat flow, but on assumption that balls behave as a round tube between two races. Mitrović *et al.* [6] presented results for the influence of temperature on the bearings' main parameters in the stationary period. Miltenovic *et al.* [7] performed a similar experiment but on assumption that heat is being generated evenly in all segments of inner and outer raceway. Takabi [8] used lumped-mass model, while this paper solves the same problem with FEM. Isert [9] used MATLAB software to create a basic code which provides a first-order approximation of the heat transfer capabilities of a bearing at low Reynolds numbers. Wang *et al.* [10] investigated the thermal feedbacks of a spindle-bearing system with measurable and adjustable bearing preload and their influence on shaft stiffness.

The level of heat generated in the bearing depends on the vertical load of the belt conveyor per one idler frame and transport speed. During the operation, shaft is stationary and only oscillates with the roller, but the outer ring, the shell and the rolling elements perform rotation. The significant majority of heat released in the idler's bearing is generated in the upper half of the bearing on the contact surfaces between the rolling elements and raceways of the inner and the outer ring. Also, during warm summer days, the outer surface of the upper part of wing idler is exposed to sun rays, while other parts of the idler frame are partially isolated by the rubber belt and transported material – coal.

In case of conventional idlers, housing and shell are made of steel, so the released heat is being performed to the environment through the housing, shell and shaft with constant heat conductivity coefficient. Idlers with housing and shell made of polymer material, have conductivity coefficient significantly lower than in a case with those who's housing and shell are made of steel. The shaft remains the only element in the assembly which can successfully remove heat away from the friction zone. The consequence is that the released heat remains in the bearing for longer period of time, which increases the temperature of the bearing. On other hand, polymer housing and shell act as insulation from the environment. This effect has dual consequence: in hot summer days it prevents Sun radiation from increasing the temperature of the assembly, and in cold winter days it disables the heat to leave the friction zone.

Since the quantity of the released heat in case of new idler is relatively small, winter operating conditions will have no adverse influence on idlers' performance. However, it is difficult to determine the role of polymer material in summer full load operating conditions, so this paper will use experimental and FEM method to find the solution to this problem.

The bearing used for the tested idlers is SKF's radial bearing 6310 with C03 internal gap tolerance. This is maximum gap tolerance and it is used in these operation conditions because the environment is polluted with dirt and dust particles, and often moisture and containing corrosion particles. External load is being distributed to the rolling elements which form the load distribution angle with the bearing's center axis which is  $\alpha < \pi$  [11].

### Released heat

The quantity of released heat depends on the vertical load, rotation speed and rolling friction coefficient. To determine the acceptable value of the rolling friction coefficient, the analysis will start from the values given in DIN 22112-2 [12] standard for idlers in coal mining industry.

According to DIN 2212-2, the idler is, as a part of the test, exposed to radial vertical force of  $N = 500$  N. It rotates at the speed of  $n = 650$  min<sup>-1</sup> and maximum resistance tangen-

tial force which can be measured on the shell surface of the reliable idler is  $F_r = 2.6$  N. This force is the consequence of internal frictional resistance, so the given value can be used as the upper limit for rolling friction coefficient calculation. The bearing mounted in the idler, SKF 6310, has diameter of the inner and the outer raceway of  $\varnothing 60.95$  mm and  $\varnothing 99.05$  mm, respectively, (data taken from MESYS engineering consulting software – Rolling Bearing Calculator). For these data the internal frictional resistance coefficient is 0.015. For comparison, the value used for calculation in [7] with radial load of 4600 N is 0.08.

To define the temperature field in the transient and stationary period, it is essential to discuss the process of heat generation. The contact area between the surface areas of the rolling elements and raceways has the shape of ellipse. The contact area is not stationary in time, and it moves as the idler rotates. The contact area on the rolling elements rotates around the axis of rotation of the rolling element. While the rolling element is in the upper zone of the bearing, it moves from the position of low to maximum radial load, and then again towards low radial load. In the position below the angle of load distribution, the rolling element is not exposed to load, so in that zone it transfers accumulated heat to the surrounding parts of the assembly. The outer ring rotates faster than the cage with rolling elements. When a certain point on the raceway enters the load distribution zone, heat generation alternates from low value to zero (when the point is between two rolling elements), and then rises again, but now to a higher level of heat generation, as the point gets closer to the center of load distribution zone, or to a lower level if point moves away from the center of load distribution zone. Depending on the current position of the rolling elements, every point of the raceway has its own oscillation of generated heat between zero, and the highest possible heat generation for that specific point. When the point leaves the zone, it transfers accumulated heat to the rest of the assembly. The inner ring raceway and shaft are fixed, so heat is being generated only on the surface of the raceway in the load distribution zone, and it alternates from low level of heat generation to zero in wing sections of the zone, or from zero to maximum heat generation in the middle of the zone.

The frequency of load intensity change is very high because it is the product of multiplication of two factors: rotational speed and number of rolling elements in load distribution zone, and it is over 40 Hz. It indicates, that after the cold start of rotation, heat generation and temperature in every point in few seconds is uniform through the whole surface of the rolling elements and the outer ring raceway. It means that many times per second, very short periods of heat generation and cooling alternate, which leads to conclusion that heat generation can be averaged for every point individually.

### Analytical calculation

Vertical load data of  $R = 3073$  N was taken from the study [13]. It presents the expected load per bearing on the horizontal idler in the period when the conveyor operates in full capacity and rotates with the constant speed of  $n = 600 \text{ min}^{-1}$ .

Friction force,  $F_{tr}$ , produces work which equals:

$$A = M \theta = F_r r_r \theta \quad (1)$$

With assumption that all produced work transforms into heat, heat flow  $\dot{Q}$  [W] equals:

$$\dot{Q} = \frac{A}{t} = F_r r_r \frac{\theta}{t} = F_r r_r \omega = (R\mu) r_r \frac{2n\pi}{60} = (3073 \cdot 0.015) 0.04 \frac{2\pi 600}{60} = 116 \text{ W} \quad (2)$$

Total produced heat flow divides into three directions towards the surrounding air, fig 1. First direction  $\dot{Q}_1$  is by conduction through the outer ring and housing and convection to environment air, second direction  $\dot{Q}_2$  is by conduction through the inner and the outer ring to bearing sides and by the convection to surrounding air, and third direction  $\dot{Q}_3$  is by conduction through the inner ring and shaft and convection to surrounding air and to air inside the shell.

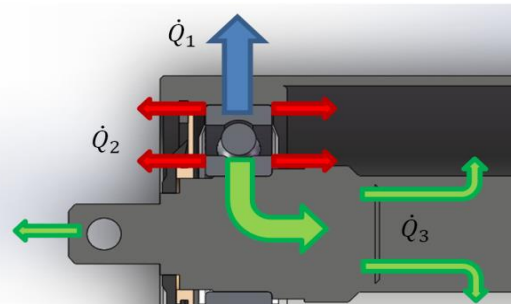


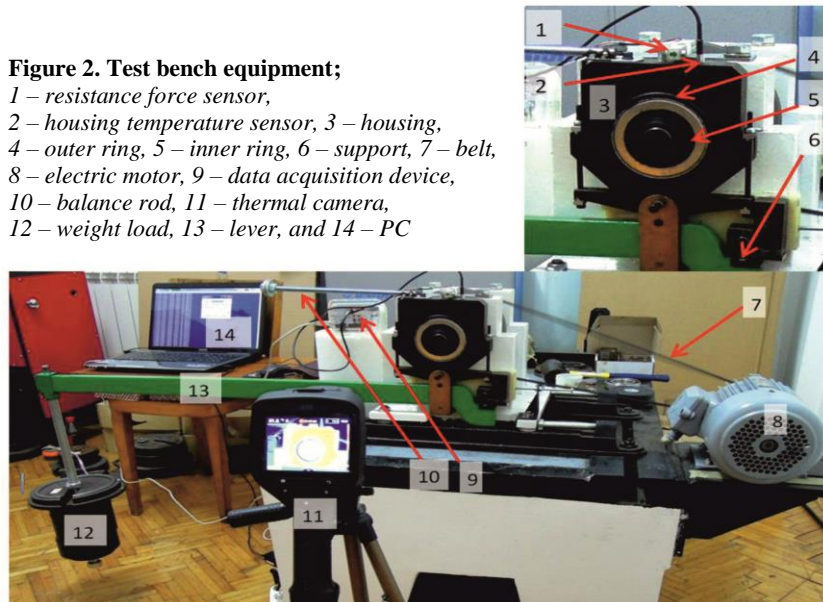
Figure 1. Heat flow distribution

### Experimental test equipment specification

The test equipment shown in fig. 2 was used to measure temperature field in the housing-bearing-shaft assembly and to measure bearing internal resistance force. Inspired by the test bench presented in [14, 15], test bench was created based on existed equipment in laboratory LIMES with new constructed and produced parts for this experiment. Eighteen tests were performed in total. Half of those were made with the housing made of steel, and the other half with the housing made of polymer. Three different rotating speeds and three different levels of load were applied to measure the influence of these physical variables on heat generation.

Figure 2. Test bench equipment;

- 1 – resistance force sensor,
- 2 – housing temperature sensor, 3 – housing,
- 4 – outer ring, 5 – inner ring, 6 – support, 7 – belt,
- 8 – electric motor, 9 – data acquisition device,
- 10 – balance rod, 11 – thermal camera,
- 12 – weight load, 13 – lever, and 14 – PC



Two different materials (polymer, steel) were used to determine the influence of housing material on temperature field in housing, bearing and shaft, under same rotational speed and load conditions. Unlike the real idler where the shaft is fixed while the housing rotates, the experimental equipment has fixed housing and rotating shaft.

The test equipment consists of: Flir E53 thermal camera, weight load, lever, support, balance rod, housing, SKF 6310 bearing, shaft, belt, electric motor, temperature sensor, force

sensor, acquisition equipment, and PC. Sensor Arduino 10 kg was used to measure internal resistance force together with HX711 24bit signal amplifier. Ambient temperature was measured with LM35CZ sensor (from  $-40\text{ }^{\circ}\text{C}$  to  $+110\text{ }^{\circ}\text{C}$  temperature range,  $+10\text{ mV/K}$ ). Housing temperature was measured with DS18B20+ KIT, Digital Thermometer, 1-Wire,  $\pm 0.025\text{ }^{\circ}\text{C}$ , 12bit. Acquired data processing was performed by software made for Arduino UNO R3-ATmega328-16MHz microcontroller.

The results were captured by Flir E53 thermal camera and thermal sensor placed in the housing near the bearing outer ring. Temperature was also checked by the contactless thermometer to estimate heat conduction through the shaft.

Balance rod was used to adjust start position of the housing, because it had a tendency to lean after being exposed to heavy weight, due to small inaccuracy in symmetry.

Three applied rotation speeds were: operational rotating speed of conveyor idler at open coal mine in Kostolac ( $600\text{ min}^{-1}$ ), 50% higher speed then operational speed ( $920\text{ min}^{-1}$ ), and almost 100% higher speed then operational speed ( $1100\text{ min}^{-1}$ ). Three weight loads (10.2 kg, 23.35 kg, and 50.58kg) were applied on the lever's end to produce radial force on the bearing of 1536 N, 3073 N, and 6146N, respectively, where 3073 N is the average operational load of the conveyor per one bearing in horizontal idler commonly used for calculations [13].

To present the influence of the housing material, the results of the measurements and calculations of temperature fields for the case of working load  $R = 6146\text{ N}$  and the rotating speed  $n = 920\text{ min}^{-1}$  were singled out. Based on the measured rotational resistance force, the friction moment is calculated and presented in the chart shown in fig. 3. Average generated heat flow of  $70.5\text{ W}$  was used for numerical calculations.

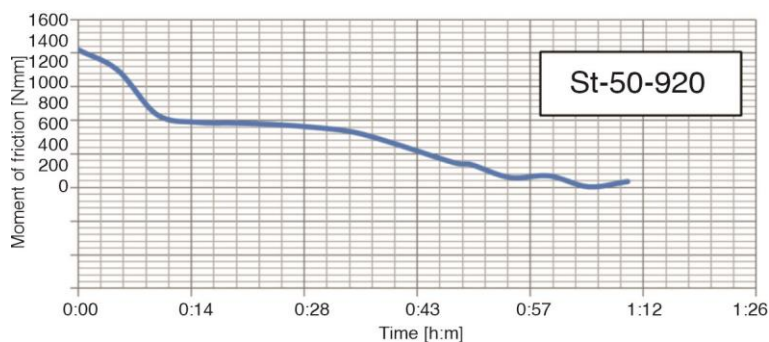


Figure 3. Moment of friction data

Figures 4(a) and 4(b) show the temperature field after 1 hour and 10 minutes of testing on the surface of the bearing assembly on the test bench measured by a Flir thermal camera.

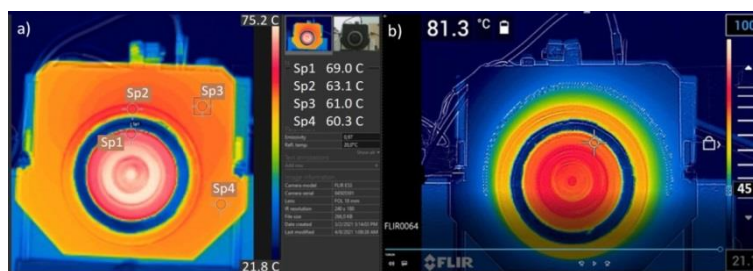


Figure 4. Thermal field results for steel (a) and polymer (b) housing,  $6146\text{ N}/920\text{ min}^{-1}/3900\text{ seconds}$

In addition to the color scale for the temperature assessment, local readings (Sp1, Sp2, Sp3, and Sp4) were made at the locations of the inner and outer bearing rings and at the housing made of steel at the location of the DS18B20 temperature sensor. The read values are shown on the right side of fig. 4(a).

Flir E53 thermal camera Accuracy:  $\pm 2\%$  of the reading at ambient temperature of 15-35 °C (59-95 °F), and object temperature above 0 °C (32 °F) (*i.e.*  $\pm 1.38$  °C for the described test with  $T_{sp1} = 69$  °C) [16].

A similar temperature field measurement was made for the polymer housing. Figure 4(b) shows a scale with the marked temperature of 45 °C. The Iso lines in the picture show the surface with this temperature. This surface overlaps with the zone in which the temperature sensor DS18B20 is located.

It is visible that the temperature in the same zone in the case of polymer housing is at least 15 °C lower than in the case of steel housing, while the bearing inner ring has 12 °C higher temperature in the case of housing made of polymer.

Delay of temperature increase in the polymer housing was noticed approximately in the first 5-10 minutes of every test, fig. 5, while the bearing and the shaft experienced rapid temperature increase. It is explained with the low level of heat conduction between the steel outer ring and the polymer housing, as long as the ring does not increase its dimensions due to the rise of the temperature, thus eliminating the micro gaps between these two surfaces.

The thermal camera confirmed the existence of the temperature field which is not symmetrical in reference to the vertical plane of shaft longitudinal axis [17]. The temperature symmetry plane is rotated for few degrees in direction of shaft rotation, fig. 4(a).

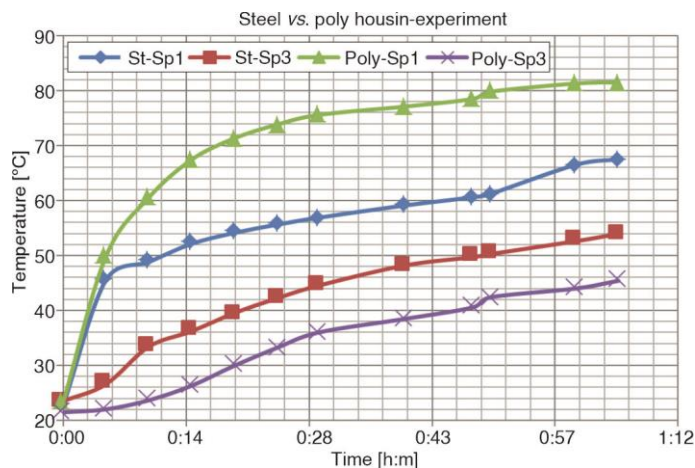


**Figure 5. Comparative results for steel and polymer housing for Sp1 and Sp3 nodes**

### Numerical method

The goal of this analysis is to create a model which can confirm the presented experimental data, and to estimate average heat convection coefficient for polymer and steel material towards the air. Heat is generated in the bearing as a consequence of friction at contact points between rolling elements and inner and outer ring raceways.

To simplify the numerical model, the rolling elements were replaced with the artificially made body, fig 6(a), having the shape of irregular ring, which generates heat and con-

nects those points of the inner and outer ring raceways that are in contact with the rolling elements in the real operational conditions. The size of the contact surface between the artificial body and the raceway is in every point equal to dimensions of Hertz contact pressure ellipse (12-3,14-11) (obtained from Hertzwin 3.1.1. software [18]) and the time of the specific point's exposure to contact pressure from any of eight rolling elements. Generated heat is the same as the one generated in the real bearing and its distribution is proportional to the size of the contact surface between the body and the raceway, fig 6(b) (red color presents the contact zone on the outer raceway and the green on the inner raceway).

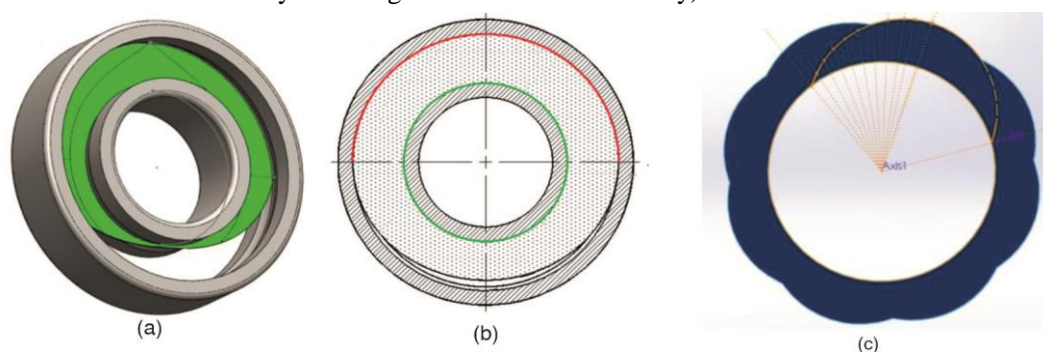


**Figure 6. Artificially body for numerical calculation; (a) shape and size, (b) contact zones, and (c) single rolling element load distribution zone**

The outer ring raceway is exposed to the pressure only in its' upper half, and the pressure in every specific point of the raceway depends on the load distribution angle and the time of the specific point's exposure to the pressure from any of the eight rolling elements. In order to enable all rolling elements to at least once make contact with the outer ring in the load distribution zone, the shaft has to make more than one revolution.

Dimensions of tested SKF 6310-2Z bearing (MESYS engineering consulting software – Rolling Bearing Calculator) are:

- Diameter of rolling element (8 pieces) 19.05mm.
- Diameter of cross section of inner and outer raceway 19.81 mm.
- Diameter of inner raceway 60.95mm.
- Diameter of outer raceway 99.05mm.

If we exclude sliding, according to the previously given dimensions, in order to make one revolution around the central bearing axial axis, the rolling element has to make 5.2 revolutions around its own axis. In the same period of time, the shaft and the inner ring make 1.63 revolutions around the central axial axis. It means that every specific point on the inner raceway is 1.63 times more often exposed to load than any specific point on the outer raceway.

The inner raceway can be exposed to load in every specific point of circumference, whenever that specific point is in the upper half of the bearing. Two points of the rolling element and the inner raceway, which are in mutual contact on the beginning of the load distribution zone, have different rotational speeds around the central axis. While the rolling element gets to the position of maximal load (90° rotation starting from the position where it enters the load distribution zone), the specific point of the inner raceway makes rotation of 146.7°, which leads to conclusion that the angle of the load distribution zone caused by the single rolling element, fig 6(c), on the inner raceway is:

$$2(146.7^\circ - 90^\circ) = 113.4^\circ \quad (3)$$

Eight rolling elements, one by one, enter the load distribution zone with  $45^\circ$  angular distance and they transfer load to the inner race. After the inner ring and the shaft perform 1.63 of the single rotation, the first rolling element is positioned again on the entrance to the load distribution zone. During the first rotation of the rolling element, each point of the inner ring was exposed (by two or three rolling elements) to about 40% of nominal load. Since there exists sliding, at revolving speed of  $600 \text{ min}^{-1}$ , one cycle lasts less than one second, it means that in the very short period of time the load on every point of the inner race will be equalized.

The conclusion is that the ideal shape of artificial body, concerning heat generation and transfer is:

- Width of the contact surface at the inner ring race is constant around its circumference and the area is 1.63 times bigger than the contact surface area at the outer ring race.
- Width of the contact area at the outer ring race is the biggest at the highest point (pos.  $\pi/2$ ) and it decreases to zero value in positions 0 and  $\pi$ . Width at the highest point responds to the width of Hertz pressure ellipse, and it is about 1 mm. Data used for analysis are presented in tab. 1.

**Table 1. Input data for thermal analysis**

Generated heat flow	70.5 W	Ambient temperature	20 °C
Coefficient of heat transfer to the environment	5 W/m <sup>2</sup> K	Radial load	6146 N
Heat conduction coefficient- Steel	43 W/mK	Rotation speed	925 min <sup>-1</sup>
Heat conduction coefficient- Poly	0.2 W/mK		

Large differences in the values of the friction coefficient were noticed in the reference papers. If the equation presented in analytical calculation is used to calculate friction coefficient (based on heat generation which creates temperature field similar to one obtained in experiment) the value of friction coefficient is 0.0045. The value is similar to one given for the idler in DIN 22112-2 (0.015) [12], as well as to value given in the bearing catalogue [19] (0.002 for new bearing).

The results of the numerical analysis are presented in fig 7(a) (steel housing) and fig 8(a) (polymer housing), after the thermal stationary stage is achieved. Elapsed time for the steel housing is 3600 seconds, and for the polymer housing is 5000 seconds. Temperature diagrams for singled out nodes are presented in fig 7(b) and fig 8(b). The singled out nodes are positioned on the inner ring lateral surface, the outer ring lateral surface and the housing surface at the position of temperature sensor.

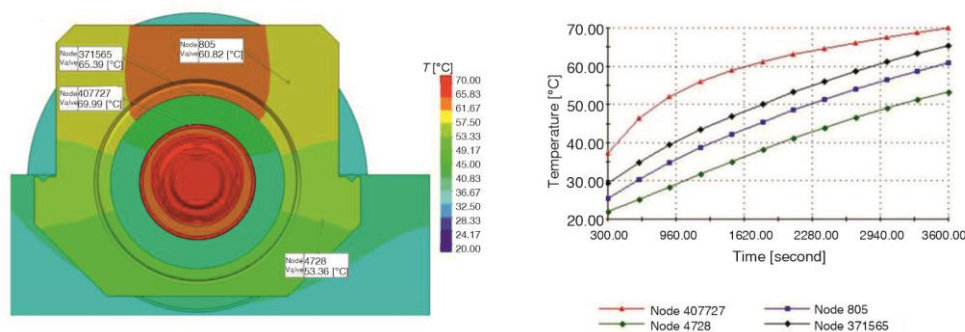


**Figure 7. Thermal field results for steel housing, 6146 N/920 min<sup>-1</sup>/3600 seconds**

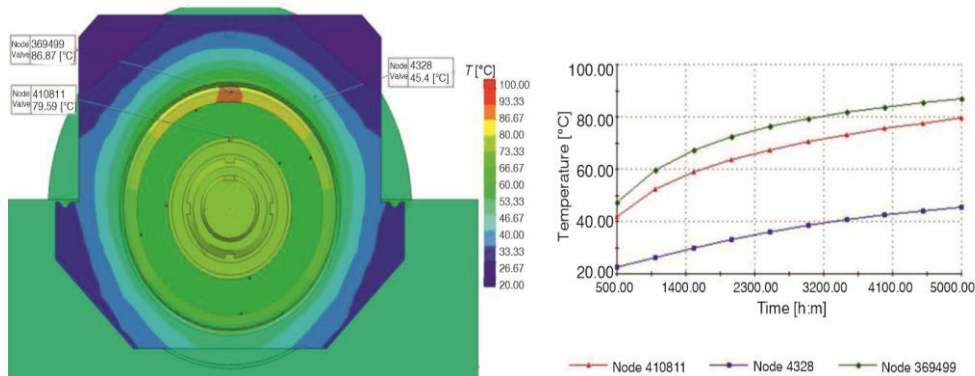


Figure 8. Thermal field results for polymer housing, 6146 N/920 min<sup>-1</sup>/3600 seconds

Diagrams on figs. 9(a) and 9(b) present comparison of FEM and the experimental results for the temperature rise in time for two characteristic nodes (inner ring lateral surface and housing surface at the position of temperature sensor). Standard result deviation is 5-10%.

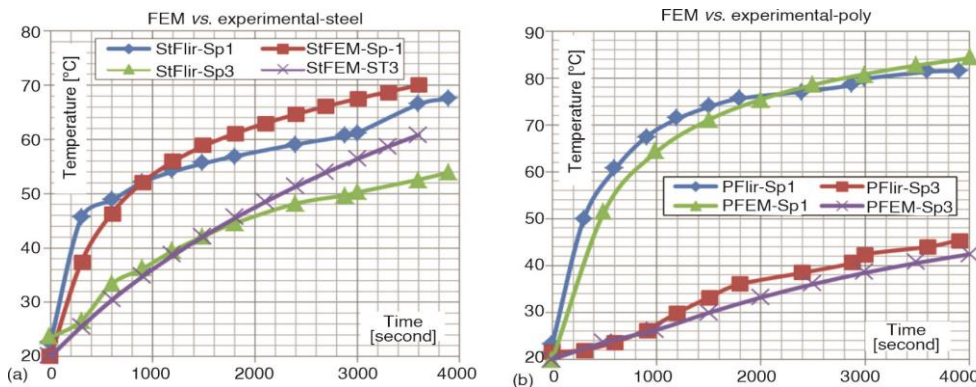


Figure 9. Thermal field results for steel (a) and polymer (b) housing; 6146 N/920 min<sup>-1</sup>/4000 seconds

The mesh density of the finite elements adapted for the construction is divided into two zones, local (fig. 6 – red and green line) and global (rest of the assembly). In order to check the convergence of the solution for the reference temperature for node 371565, three FEM models of steel housing shown in tab. 2 were created. The last FEM model was adopted and used for the PA model as well.

Table 2. Convergence of the solution for node 371565 temperature

Mesh element size		Number of nodes	Number of elements	Node 371565 temperature
Global	In contact zones			
10 mm	0.5 mm	423.363	248.539	65.14 [°C]
8 mm	0.5 mm	528.426	320.343	65.24 [°C]
4 mm	0.5 mm	1.664.314	1.118.740	65.39 [°C]

## Conclusion

The thermal consequences of polymer material usage for construction of housing and shell of conveyor belt idlers were tested in two ways: by using numerical method and

experiment. This paper proves that the results close to heat generation zone obtained in all the tests had similar values with accuracy of 5-10%. The experimental results captured with the thermal camera confirmed that the temperature field has tendency as expected by numerical simulation made by FEM numerical analysis in SolidWorks Simulation [20]. Maximum temperature of polymer housing at measurements point for test with maximum radial load and rotation speed of  $920 \text{ min}^{-1}$  was below  $45 \text{ }^\circ\text{C}$ , while the temperature of the inner ring was below limit values for lithium grease from  $120 \text{ }^\circ\text{C}$  [20]. This confirms that the usage of polymer in construction of conveyor belt idlers has no unfavorable impact in terms of overheating of the bearing.

## References

- [1] Yan, L., *et al.*, Investigation Into the Effect of Common Factors on Rolling Resistance of Belt Conveyor, *Advances in Mechanical Engineering*, 7 (2015), 8, pp. 1-34
- [2] Harris, T. A., *Rolling Bearing Analysis*, 4<sup>th</sup> ed., John Wiley & Sons, New York, USA, 2001
- [3] Živković, A., *et al.*, Software Solution for Analyzing the Behavior of Ball Bearings - Technical Solution (in Serbian), Ph. D. thesis, University of Novi Sad, Faculty of Technology, Novi Sad, Serbia, 2013
- [4] Azianou, A. E., *et al.*, Modeling of the Behavior of a Deep Groove Ball Bearing in Its Housing, *Journal of Applied Mathematics and Physics*, 1 (2013), 4, pp. 45-50
- [5] Kushwaha, A. S., *et al.* Analysis of the Ball Bearing Considering the Thermal (Temperature) and Friction Effects, *Proceedings, National Conference on Emerging Trends in Engineering & Technology Chennai, India*, pp. 115-120
- [6] Mitrović, R., *et al.* Effects of Operation Temperature on Thermal Expansion and Main Parameters of Radial Ball Bearings, *Thermal Science*, 19 (2015), 5, pp. 1835-1844
- [7] Miltenovic, A., *et al.* Prediction of Heat Generation in Transmission Bearings by Application of FEM, *Proceedings, International VDI Conference on Gears, Munich, Germany, 2017*
- [8] Takabi, J., On the Thermally Induced Failure of Rolling Element Bearings, Ph. D. thesis, Louisiana State University and Agricultural and Mechanical College, Baton Rouge, La., USA, 2015
- [9] Isert, S., Heat Transfer Through A Rotating Ball Bearing At Low Angular Velocities, M. Sc. Thesis, All Graduate Plan B and other Reports.90, Utah State University, Logan, Ut., USA, 2011
- [10] Wang, H., *et al.*, A Dynamic Thermal-Mechanical Model of the Spindle-Bearing System, *Mech. Sci.*, 8 (2017), 2, pp. 277-288
- [11] Kostić, S., *et al.*, Analysis of the Influence of Internal Radial Clearance on the Load Distribution of the Rolling Ball Bearing, *Mobility & Vehicle Mechanics*, 45 (2019), 2, pp 15-25
- [12] \*\*\*, DIN 22112-2, Belt Conveyors for Underground Coal Mining - Idlers-Part 2: Requirements
- [13] Tasić, M., Mitrović, R., The Project of Realizing the Reliability of the Operation of Rollers on Transport Systems with Special Reference to the Examination of the Operation of the Rollers in Exploitation Conditions - Part C (in Serbian), Faculty of Mechanical Engineering, University of Belgrade, Belgrade, 2010
- [14] Wang, Y., *Et Al.*, Investigation On Frictional characteristic of Deep-Groove Ball Bearings Subjected to Radial Loads, *Advances in Mechanical Engineering*, 7 (2015), 7, pp. 1-12
- [15] Ionut Geonea, I., *et al.*, Experimental and Theoretical Study of Friction Torque from Radial Ball Bearings, *IOP Conference Series Materials Science and Engineering*, 252 (2017), 012048
- [16] \*\*\*, FLIR E53, <https://www.flir.com/products/e54/>
- [17] Mišković, Ž. Z., Exploitational Contamination Particles Concentration Influence on Rolling Bearing's Operational Characteristics (in Serbian), Ph. D. thesis, University of Belgrade, Faculty of Mechanical Engineering, Belgrade, Serbia, 2017
- [18] \*\*\*, Hertzwin 3.1.1, <https://www.vinksa.com/toolkit-mechanical-calculations/hertz-contact-stress-calculations/>
- [19] \*\*\*, FKL Rolling Bearings, catalog, FKL Temerin
- [20] Weber, M., SolidWorks Simulation 2017-Black Book, CAD/CAM/CAE Works, USA, 2016